



HAL
open science

Macroplastic transfer dynamics in the Loire estuary: Similarities and specificities with macrotidal estuaries

L. Ledieu, R. Tramoy, D. Mabilais, S. Ricordel, L. Verdier, B. Tassin, Johnny Gasperi

► To cite this version:

L. Ledieu, R. Tramoy, D. Mabilais, S. Ricordel, L. Verdier, et al.. Macroplastic transfer dynamics in the Loire estuary: Similarities and specificities with macrotidal estuaries. *Marine Pollution Bulletin*, 2022, 182, pp.114019. 10.1016/j.marpolbul.2022.114019 . hal-03755097

HAL Id: hal-03755097

<https://enpc.hal.science/hal-03755097>

Submitted on 22 Aug 2022

HAL is a multi-disciplinary open access archive for the deposit and dissemination of scientific research documents, whether they are published or not. The documents may come from teaching and research institutions in France or abroad, or from public or private research centers.

L'archive ouverte pluridisciplinaire **HAL**, est destinée au dépôt et à la diffusion de documents scientifiques de niveau recherche, publiés ou non, émanant des établissements d'enseignement et de recherche français ou étrangers, des laboratoires publics ou privés.

1 **Macroplastic transfer dynamics in the Loire estuary:** 2 3 4 **similarities and specificities with macrotidal estuaries**

5
6
7 L. Ledieu¹, R. Tramoy^{2,3}, D. Mabilais¹, S. Ricordel¹, L. Verdier¹, B. Tassin^{2,3}, J. Gasperi¹

8
9 ¹ Univ Gustave Eiffel, GERS-LEE, F-44344 Bouguenais, France.

10 lauriane.ledieu@univ-eiffel.fr; johnny.gasperi@univ-eiffel.fr

11 ² Univ Paris Est Créteil, LEESU, F-94010 Créteil, France.

12 ³ Ecole des Ponts, LEESU, F-77455 Champs-sur-Marne, France.

13 **Abstract**

14 The quantification of macroplastic fluxes transferred by rivers toward the pelagic environment requires a better
15 understanding of macrodebris transfer processes in estuarine environments. Following the strategy adopted in the
16 Seine estuary, this study aims to characterize macroplastic trajectories in the Loire estuary. Between January 2020
17 and July 2021, 35 trajectories were monitored using plastic bottles equipped with GPS-trackers. With total
18 travelled distances between 100 m and 103.6 km, trajectories show great spatiotemporal variability. The various
19 forcing factors (macroplastic buoyancy, estuaries tidal and hydrometeorological conditions, geomorphology and
20 vegetation) lead to chaotic trajectories, preventing accurate predictions in macroplastic transfer and
21 storage/remobilization dynamics. In the Loire estuary like in the Seine one, no tracked bottle reached the Atlantic
22 Ocean. It confirms that macrotidal estuaries under temperate climates constitute accumulation zones and slow
23 pathways for macroplastics, but raises question on the real fluxes transferred from continental areas to oceans.

24 **Keywords:** Storage, remobilization, GPS, buoyancy, geomorphology

25 **1. Introduction**

26 The negative impact of anthropogenic litter, especially macroplastics, has been largely enounced (van
27 Emmerik and Schwarz, 2020; Vegter et al., 2014) and become an increasing topic of interest in environmental
28 sciences. Rivers were pointed out as major pathway for macroplastics (Bruge et al., 2018; Lechthaler et al., 2020;
29 Schmidt et al., 2017). As estuarine environments are at the land-ocean interface, it is crucial to know how these
30 complex systems contribute to plastic dynamics at this interface. Like for other pollutants, the challenge is to know

28 if estuaries constitute sink or sources (Schöneich-Argent et al., 2020; Vermeiren et al., 2016) but few studies deal
29 with macroplastic transfer and accumulation in these environments (van Emmerik and Schwarz, 2020; Mazarrasa
30 et al., 2019; Pinheiro et al., 2021; Tramoy et al., 2020a, b).

31 Within rivers, the transfer of macroplastics over short spatiotemporal scales is driven by hydrometeorological
32 conditions namely water level, current velocity and flow (van Emmerik et al., 2020a; van Emmerik and Schwarz,
33 2020) as well as inherent characteristics of macroplastics like their shape, size, mass and composition, affecting
34 their buoyancy and thus their mode of transportation (Vermeiren et al., 2016). Estuaries are actually complex
35 systems with (i) a strong influence of wind speed and direction (Browne et al., 2010; Rech et al., 2014), (ii) the
36 adding role of tides (Sadri and Thompson, 2014), (iii) the influence of atmospheric pressure on water levels
37 (Tramoy et al., 2020b), and (iv) the variable hydrological conditions along the estuarine gradient (Possatto et al.,
38 2015) with the presence of the Turbidity Maximum Zone (TMZ; Vermeiren et al., 2016). The complex interactions
39 of these processes lead to chaotic dynamics depending on many parameters (e.g. tidal and hydrometeorological
40 conditions, estuarine gradients). Because of this complexity, the spatiotemporal evolutions and residence time of
41 macroplastics are difficult to quantify and remain poorly understood (Tramoy et al., 2020a; van Emmerik et al.,
42 2022).

43 Meijer et al. (2021) estimated an annual amount of macroplastics entering the oceans between 0.8 and 2.7
44 million metric tons and González-Fernández et al. (2021) between 1 656 and 4 997 metric tons at the European
45 scale. Estimations on the basis of statistics and conceptual models however show large discrepancies with field
46 observations (Castro-Jiménez et al., 2019; Dris et al., 2020; González-Fernández et al., 2021). Moreover, among
47 the few investigations of macroplastic transport and accumulation in estuarine systems, methodological
48 dissimilarities make most of the time the results difficult to compare (Dris et al., 2020). New technologies currently
49 developed make these applications easier. For example, remote sensing were used to draw the distribution of
50 plastic litter from local to global scales (Duncan et al., 2020) but especially in marine environments (Biermann et
51 al., 2020; Maximenko et al., 2019). In environments at land-ocean interfaces, Duncan et al. (2020) and Tramoy et
52 al. (2020a) demonstrated a good capacity to follow the macroplastic transfer dynamics at short spatiotemporal
53 scales by using GPS tracking bottles in the Ganges delta and the Seine estuary, respectively.

54 In the Seine estuary, Tramoy et al. (2020a, b) showed back and forth movements as well as
55 storage/remobilization processes leading to a long residence time of macroplastics, up to decades. These results

56 suggest that estuarine systems mainly act as accumulation zones and thus as slow pathways releasing low amounts
57 of plastics to the ocean. But, is this behavior general or site-specific?

58 This paper proposes a comprehensive approach of macroplastic transfer and accumulation dynamics
59 along the Loire estuary. To help discussing the analogies and specificities of the Loire estuary, the same
60 methodology than Tramoy et al. (2020b) was used by the release of bottles equipped with GPS-trackers. This study
61 aims to (i) provide a site-specific comprehension of the fate of macroplastics within the Loire estuary for a better
62 management of this contamination, (ii) confirm the role of tidal and hydrometeorological conditions by the
63 monitoring trajectories between January 2020 and July 2021, (iii) assess the influence of buoyancy by the release
64 of paired bottles: one floating and one ballasted and (iv) discuss the role of estuarine specificities in the
65 macroplastic transfer and accumulation on the basis of two feedbacks from the Seine and the Loire estuaries.

66

67 **2. Material and methods**

68 **2.1. Loire River estuary**

69 The Loire River is 1 006 km long and drains about 20% of the French territory (Sellier, 2012; Figure 1b).
70 Its estuary starts at Ancenis, 97 km upstream the river mouth (Figure 1c) and is the second largest of the French
71 Atlantic coast (SNPN, 2008). At the estuary entrance, water flow ranges from around 100 m³/s to more than 6 000
72 m³/s (mean water flow equals to approximately 850 m³/s at Montjean sur Loire; Sellier, 2012). Worldwide,
73 different types of estuaries exist according to their tidal ranges (micro-, meso- and macrotidal, Figure 1a). With
74 tidal ranges up to 6 m (Boët et al., 2011), the Loire estuary is qualified as macrotidal (Figure 1a). The extension
75 of the Turbidity Maximum Zone (TMZ) is variable according to water flows and tidal ranges (GIP, 2014). TMZ
76 extends at least until the kilometeric point (pk) 15 and at most until pk 66 (GIP, 2014; Figure 1c).

77 In its estuarine part, the Loire River is bordered by tilted blocks constituting staggered plateaus and
78 hillsides at low elevations. It is therefore characterized by a flat topography which appears symmetric from North
79 to South (Figure 1c). These steps-shaped riverbanks lead to the formation of the most diverse wetlands of France
80 (6.5% of its surface; SNPN, 2008; Figure 1c) which are managed and protected (SAGE, 2020) for their high
81 ecological value. This is particularly the case for reedbeds, covering between 2 300 and 2 800 ha (GIP, 2016).
82 Wetlands downstream from Nantes (Figure 1c) also constitute significant submersible areas (SAGE, 2020).

83 With the presence of Nantes agglomeration (sixth most populated city in France), more than 1 million of
84 people lived in the part of the Loire watershed from Ancenis to the rivermouth (3% of the total watershed surface)
85 in 2016 (SAGE, 2020). Nevertheless, along the estuary, the landcover is mainly composed of agricultural lands
86 (Figure 1c). Because of the port activities of St-Nazaire and Nantes, the Loire estuary has undergone many
87 modifications: channeling, containment, enrockment as well as the construction of hydraulic (e.g. herringbones)
88 and navigation structures (Sellier, 2012). As a result, the Loire estuary is slightly meandered (sinuosity index of
89 1.1) contrary to the Seine River (sinuosity index of 1.9). Moreover, the estuary flares towards the river mouth,
90 passing from a width of 200 m upstream, to about 15 km at the river mouth (Sellier, 2012; Figure 1c).

92 **2.2. Tracker program and data collection**

93 To perform the monitoring, the same customized tracked bottles than Tramoy et al. (2020b) were used. It
94 consists of 1 L plastic bottles, commonly used for water sampling and made of HDPE, equipped with GPS-trackers
95 (©INETIS). In order to ensure waterproof conditions and a good transmission, very compact GPS-trackers were
96 chosen to be easily placed in the bottles without playing a key role in their buoyancy. The INET-OS operating
97 system of these GPS-trackers is configurable, which makes possible to set a tracker program adapted for this study.
98 Moreover, the GPS-tracker contains accelerometers enabling to save battery energy through a standby mode. In a
99 perspective of reproducibility, the tracker program defined by Tramoy et al. (2020b) was used, program available
100 on request. The program uses grafcet language and was programmed with three states: “state 0” when the tracker
101 is off, “state 1” when the program starts after motion detection or clock setting, and “state 2” when the program is
102 on standby after 14 h without motion. During state 1, the tracker records one position every 2 h to get several
103 positions during a tidal cycle (12 h) for 33 trajectories. Moreover, 2 trajectories were recorded with a higher
104 temporal resolution, i.e. one position every 30 min. State 2 aims to save battery energy during stranding episodes
105 longer than one tidal cycle. However, the program goes back to state 1 when the tracker detects motion again.
106 Recorded positions were sent once a day to a server with a GSM/GPRS system.

108 **2.3. Experiment design**

109 Except for the influence of bottle’s buoyancy, it was chosen to adopt a stochastic approach to observe
110 bottles trajectories, i.e. by the release of bottles at different locations of the estuary and during different conditions

111 of water flow and tidal range, and to describe them through a Lagrangian description. Between January 2020 and
112 July 2021, 35 trajectories were therefore monitored in the Loire estuary (Table S1). The locations of release are
113 mapped in Figure 1c and detailed characteristics of each location are in Table S1: 10 were released upstream
114 Nantes in the estuarine-fluvial zone of the estuary and 25 were released in the internal estuary, including 19 in
115 Nantes urban area and 6 downstream. To avoid a quick stranding on riverbanks, 46% of the bottles were released
116 in the middle of the channel from bridges (Table S1). The remaining 54% were thrown in the river from riverbanks,
117 approximately 5 m from the riverbank (Table S1). All details about initial and final conditions of the tracked bottles
118 are available in Table S1. References and information relative to the tracking experiment were tagged on bottles
119 to enhance possibilities of recovery. Nevertheless, among the 35 bottles released, 6 were definitively lost either
120 because of the loss of the signal ($n = 3$), or by accidental picking of a cleanup service ($n = 1$), or because they were
121 stuck under navigation structures ($n = 2$; Table S1). Their trajectories were however considered because the
122 program used enables to recover sent positions on the server.

123 The influence of bottles buoyancy was observed through the release of two 1L-bottles at the same time
124 and same place (57% of the trajectories, Table S1): one empty, i.e. floating, and one ballasted with sand, i.e. half-
125 submerged. “Empty bottles” had a mass ranging from 169 to 250 g (density 0.161 to 0.238, Table S1) resulting in
126 high buoyancy, lying on the water surface (16 to 24 % of the volume submerged, Table S1) and letting a significant
127 surface area subjected to wind. They are called “floating bottles”. In contrast, the ballasted bottles had a mass
128 ranging from 790 to 1 004 g (density 0.752 to 0.956, Table S1). They stayed vertical (75 to 96 % of the volume
129 submerged, Table S1) and are called “half-submerged bottles”. In this case, the GPS-tracker was maintained in the
130 emerged part of the bottle with expanded foam.

131

132 **2.4. Data treatment**

133 A trajectory represents the course of a tracked bottle in space and time between its release and its retrieval
134 (or loss). It therefore includes the water transport and the stranding episodes. The following parameters were
135 recorded: initial and final conditions, distances, speeds, stranding/remobilization episodes, and tidal and
136 hydrometeorological conditions (Table 1). Water flow data were taken at the Montjean-sur-Loire station (Figure
137 1b) on <http://www.hydro.eaufrance.fr/> and water levels, flood/ebb tides and tidal ranges were taken at the St-
138 Nazaire station on <http://maree.info/>. The trajectories were rebuilt using GPS positions processed by QGIS
139 (QGIS.org, 2022). To calculate distances and speeds, kilometric points (pk) were assigned to each GPS position.

140 These points are calculated along a virtual streamline in the middle of the channel positively oriented upstream. In
141 this study, pk 0 was set at St-Nazaire (Figure 1c). The characteristics of the stranding sites (i.e. riverbank and
142 vegetation typologies) were also reported under QGIS using the data supplied by the GIP Loire Estuaire.

143 Statistical tests were performed to rank the influence of each environmental variable (site of release, water
144 flow and tidal ranges). Statistics were performed with RStudio 1.4.1717 (RStudio Team, 2021). Respective
145 weights of influencing factors (environmental conditions and bottles buoyancy) on trajectory parameters were
146 assessed through a principal component analysis (PCA) using “FactoMineR” (Lê et al., 2008), “ggplot2”
147 (Wickham, 2016) and “factoextra” (Kassambara and Mundt, 2020) packages.

149 3. Results

150 3.1. Macroplastic transfer dynamics in the Loire estuary

151 All parameters are described in Table 1 and written in italic in the following parts. The trajectories exhibit
152 *total durations* ranging from 6 h to 64 days (median value equals to 11 days, Figure 2, Table S2). The tracked
153 bottles thus spent up to two months on field. Over the 35 trajectories, 32 show to a *total duration* longer than one
154 day. Lower *total durations* are recorded for 3 trajectories because of signal loss (T2 and T32) and accidental
155 picking of the tracked bottle by a cleaning service (T21, Figure 2, Table S2). As the recovery of the tracked bottles
156 was opportunistic, the *travel time* without considering the last stranding is therefore calculated to avoid any bias.
157 This parameter varies between ½ h and 58 days (median value equals to 14 h, Table S2) excluding T2, T21 and
158 T32. Trajectories show high spatiotemporal variabilities with *maximum speeds* ranging from 0 (immediately
159 stranded) to 32 km/h (median value equals to 4.2 km/h, Table S2) and *total distances* ranging from 0.1 to 103.6
160 km (median value equals to 10.6 km, Table S2). In comparison, *net distances* are lower, ranging from -6.4 to 59
161 km (median value equals to 6.3 km, Figure 3, Table S2). Here, negative *net distances* mean tracked bottles were
162 recovered upstream their initial location release. Nevertheless, not all trajectories exhibit a difference (Figure 3)
163 as the (*Total – Net*) *distances* range from 0 to 92.8 km (median value equals to 0.4 km, Table S2).

164 The tracked bottles *travel time in water* does not exceed 4 days (median value equals to 10 h, Table S2)
165 illustrating stranding processes occurring quite quickly. Except one (T32, bottle lost), all trajectories exhibit at
166 least one *stranding episode* longer than 12 h (Figure 2, Table S2). Between 1 and 3 *stranding episodes* were
167 monitored per trajectory showing remobilization processes (Figure 2, Table S2) but 54% of the trajectories exhibit
168 only 1 *stranding episode* (Figure 2, Table S2). Consequently, for these trajectories, the *travel time* corresponds to

169 the *travel time in water* (Table S2) and has to be taken with caution. Among the 46% of trajectories for which
170 remobilization processes occurred, the *stranding time* is between 10 h and 57 days (median value equals to 3 days,
171 Table S2). The final stranding occurred during the highest *tidal range* of the monitored period for 69% of the
172 trajectories. In total, 55 *stranding episodes* longer than a tidal cycle (12 h) and 21 *remobilization episodes* were
173 recorded. *Remobilization episodes* occurred mostly during *flood tides* (62%). Only 52% of these episodes truly
174 removed the bottles to transport them between 0.2 and 65.1 km downstream (median value equals to 8.4 km, Table
175 S3). Bottles were pushed between 0.1 and 0.2 km along riverbanks (median value equals to 0.1 km, Table S3) and
176 between 0.2 and 1.1 km farther in submersible areas (median value equals to 0.4 km, Table S3), both for 19% of
177 these episodes. For the last 10%, bottles were pushed between 0.2 and 1.4 km farther in lateral channels (median
178 value equals to 0.8 km, Table S3).

179 Considering the *riverbank and vegetation typologies*, 73% of the *stranding episodes* occurred in intertidal
180 areas (Figure 4, Table S3). Most of the tracked bottles stranded on natural riverbanks (36%), 25% on rock
181 embankments, 16% on urban riverbanks, 9% in submersible areas and 7% in lateral channels (Figure 4, Table S3).
182 Moreover, 67% of the tracked bottles were retrieved in riparian vegetation in which 54% are reedbeds and 46%
183 are other types of vegetation like meadows or woods (Figure 4, Table S3). Among the bottles stranded in the
184 riparian vegetation in the downstream part of the estuary, the *remobilization episodes* occurred rather in meadows
185 or woods (59%) than in reedbeds (41%, Figure 4, Table S3).

186

187 3.2. The impact of hydrological conditions

188 The spatiotemporal variability of the trajectories according to the initial *water flow* was observed to
189 identify general trends and considering the influence of this factor on trajectory parameters (Figure S1). With
190 *water flow* (Q_i) ranging from 408 to 4 080 m³/s (Table S2), three clusters of trajectories were designed relative to
191 the mean value ($Q_i = 1\ 248\ \text{m}^3/\text{s}$ during the 35 monitored trajectories): low hydrological conditions (LHC, $Q_i =$
192 $595 \pm 116\ \text{m}^3/\text{s}$, $n = 17$), high hydrological conditions (HHC, $Q_i = 1\ 219 \pm 237\ \text{m}^3/\text{s}$, $n = 12$) and flood conditions
193 ($Q_i = 3\ 161 \pm 827\ \text{m}^3/\text{s}$, $n = 6$, Table S2).

194 The *travel time in water* is the lowest during flood events (median value equals to 0.2 days, Figure 5a,
195 Table S4a). During these hydrological conditions, *total* and *net distances* are equal and the highest (median value
196 equals to 13.5 km, Figure 5a, Table S4a). The *maximum speeds* reached by the tracked bottles are also three times
197 higher during flood events (median value equals to 9.1 km/h, Table S4a) than during LHC and HHC (median

198 values equal to 3.3 km/h and 3.7 km/h, respectively, Figure 5a, Table S4a). During HHC, the *travel time in water*
199 (median value equals to 0.7 days) and *net distances* travelled by the tracked bottles (median value equals to 4.7
200 km) are slightly higher than during LHC (median value equals to 0.4 days and 3.9 km, respectively, Figure 5a,
201 Table S4a). An opposite trend is however observed for *total distances* (median values equal to 5.1 km and 7.8 km
202 during HHC and LHC, respectively, Figure 5a, Table S4a), which leads to higher (*Total – Net*) *distances* during
203 LHC (median value equals to 11.2 km, Figure 5a, Table S4a).

204 Trajectories exhibit a median value of 1 *stranding episode* (Figure 5a, Table S4a) and most of them
205 occurred in intertidal areas (78%, 72% and 71% for flood events, HHC and LHC, respectively, Table S3) whatever
206 the hydrological conditions. Nevertheless, the tracked bottles mostly stranded on the north *side* during flood events
207 (67%) and on the south *side* during LHC (61%, Table S3). Moreover, more *stranding episodes* occurred on the
208 Loire islands during flood events and HHC (22% and 28%, respectively) than during LHC (7%, Table S3). Because
209 of embankments and enrockments, a high proportion of bottles were retrieved in Nantes agglomeration during
210 HHC (50%) and LHC (46%) and on natural riverbanks during flood events (67%, Table S3). The percentage of
211 bottles remobilized after stranding was slightly higher during LHC (43%) than during flood events and HHC (33%
212 for both, Tables S2 and S4). Nevertheless, 83% of the *remobilization episodes* truly removed the bottles to
213 transport them elsewhere during HHC whereas this proportion falls to 42% during LHC (Table S3).

214

215 3.3. The impact of macroplastic buoyancy

216 With ten paired bottles released with different densities (D) at the same location and at the same time,
217 two clusters of trajectories were designed relative to bottle's *buoyancy*: floating (F, $D = 0.207 \pm 0.037$, $n = 10$) and
218 half-submerged (H-S, $D = 0.831 \pm 0.064$, $n = 10$). Floating and half-submerged bottles show different trajectories
219 (Figure 3). A video of a paired trajectory (T19 and T20) is available on the online version of this paper and
220 illustrates these differences. Half-submerged bottles have higher *travel time in water* (median value equals to 1.2
221 days) than floating ones (median value equals to 0.2 days, Figure 5b, Table S4b). As a result, *total and net distances*
222 travelled by floating bottles are lower (median values equal to 5.1 km and 3.2 km, respectively) than half-
223 submerged ones (median values equal to 18.4 km and 4.7 km, respectively, Figure 5b, Table S4b), which have
224 consequently the highest median value of (*Total – Net*) *distances* (equals to 6.0 km compared to 0.7 km for floating
225 bottles, Table S4b). Exceptions are however noticed with high (*Total – Net*) *distances* whatever the bottle's
226 *buoyancy*, mostly during the spring tides with the highest *tidal range* (6 m, Figure 3). Moreover, half-submerged

227 bottles have lower *maximum speeds* (maximum value equals to 5.8 km/h) than floating ones (maximum value
228 equals to 9.0 km/h, Figure 5b, Table S4b).

229 The number of *stranding episodes* is different between floating (12 episodes in total) and half-submerged
230 bottles (22 episodes in total, Figure 5b, Tables S2 and S4b). Floating bottles mostly stranded in intertidal areas
231 (75%) during *ebb tides* (67%, Table S3). In contrast, half-submerged bottles stranded as much in intertidal areas
232 (59%) than in lateral channels (18%) or in submersible areas (14%, Table S3) because these can be carried farther.
233 Their *stranding episodes* occurred mainly during *flood tides* (73%, Table S3). These bottles exhibit 12
234 *remobilization episodes* but only 7 of these episodes (58%) truly removed the bottles to transport them elsewhere
235 (Table S3). The other episodes pushed the bottles laterally on the riverbank (8%) or farther in submersible areas
236 (17%) and in lateral channels (17%) mostly during *flood tides* (75%, Table S3). In contrast, floating bottles exhibit
237 2 *remobilization episodes* and both truly removed them during *ebb tides* (Table S3). No preferential accumulation
238 zone appears between natural riverbanks, rock embankments and urban riverbanks (Table S3). Also, no trends are
239 observed between *end sites* and/or their *vegetation typologies* (Table S3).

240

241 4. Discussion

242 In agreement with the few studies performed in estuaries (Swan River (Australia), Hajbane and
243 Pattiaratchi, 2017; Paranaguá Bay (Brazil), Krelling and Turra, 2019; Pas, Miera and Asón Rivers (Spain),
244 Mazarrasa et al., 2019; Seine River (France), Tramoy et al., 2020b), the macroplastic transfer dynamics have a
245 high spatiotemporal variability in the Loire estuary (Figures 2 and 3). This variability can be explained by a
246 combination of factors. For example, *start pk* and bottles *buoyancy* are not sufficient to explain the variable *net*
247 *distances* travelled by the tracked bottles (Figure 3). It evidences that plastic debris have chaotic trajectories within
248 estuaries (Tramoy et al., 2020b) compared to their horizontal downstream transport within rivers. Forcing factors
249 are therefore hard to quantify and to rank. The multifactor character of the trajectories is illustrated by the low
250 weight of each factor (represented by the length of their arrows) in the PCA despite that the first two axes explain
251 around 70% of the data variance (Figure S1). Nevertheless, the factor having the highest weight on trajectory
252 parameters is the initial *water flow* (Figure S1). Focusing on specific physical drivers can help to highlight a better
253 picture of the dynamics of interest (Hajbane and Pattiaratchi, 2017). That's why tidal and hydrometeorological
254 conditions, macroplastic buoyancy as well as the estuarine geomorphology are discussed separately below.

255

1

2

3 256

4.1. A chaotic journey for macroplastics in the Loire estuary

4

5 257

4.1.1. A high residence time because of tides

6

7 258

8

9 259

10

11 260

12

13 261

14

15 262

16

17 263

18

19 264

20

21 265

22

23 266

24

25 267

26

27 268

28

29 269

30

31 270

32

33 271

34

35 272

36

37

38 273

39

40

41 274

42

43 275

44

45 276

46

47 277

48

49 278

50

51 279

52

53 280

54

55 281

56

57 282

58

59 283

60

61

62

63

64

65

Tides-induced processes play a key role in macroplastic travelled *distances* and residence time (Liro et al., 2020). In this work, values of (*Total – Net*) *distances* evidenced back and forth movements of the tracked bottles (Figure 2), consistently with other studies (Tramoy et al., 2020b; van Emmerik et al., 2020b). These movements derive from the bidirectional flows induced by tides and considering the maximum value of this parameter (i.e. 92.8 km), macroplastics can be easily pushed back to the upstream part of the Loire estuary. Tides also generate high variations in water levels and these variations lead to storage/remobilization processes (Tramoy et al., 2020b; van Emmerik et al., 2020b). This impact is corroborated by the increasing of both the capacity of macroplastics to strand (Kurniawan and Imron, 2019a) and debris residence time with increasing tidal ranges (section 3.1.). Moreover, Vermeiren et al. (2016) conceptualized intertidal areas as a temporary sink for macroplastics and the predominance of *stranding episodes* in intertidal areas in this study (Figure 4) confirms this concept. Debris have therefore stepwise trajectories, resulting in higher residence time within estuaries than previously thought (Ivar do Sul and Costa, 2013; Tramoy et al., 2020b; van Emmerik et al., 2020b). In the Loire estuary, the latter far exceeded the water residence time, which is between 3 and 30 days (Briant et al., 2021). Even if the tracked bottles spent up to 2 months on field and travelled up to 100 km, none of them reached the Atlantic Ocean, indicating that this estuary also constitutes an accumulation zone and slow pathway for macroplastics.

4.1.2. A significant impact of hydrological conditions

Macroplastic transfer dynamics within estuaries are also driven by the hydrological flow regime (van Emmerik et al., 2019) which drives the dominant processes between tides and river outflows (Dris et al., 2020; Tramoy et al., 2020b). Results of this study actually highlight variable dominant processes according to *water flow*. During flood events, the flushing effect of river flow-dominated processes led to a fast downstream transfer of debris over long distances (*net distances* up to 59 km, Table S4a). Despite high *tidal ranges* (up to 4.6 m, Table S2), macroplastic transfer dynamics were not affected by back and forth movements because the stranding also occurred quickly (median value of *travel time in water* equals to 0.2 days, Figure 5a, Table S4a) and even quicker when flood events occurred at *flood tides*. Consequently, as suggested by Dris et al. (2020) and van Emmerik et al. (2022), these results confirm that extreme events play a key role in the macroplastic transfer distances and residence time. Apart from extreme events, in the Loire estuary, the capacity of macroplastics to be transferred

284 downstream was in average limited whatever the hydrological conditions (median values of *net distances* equal to
1 285 3.9 and 4.7 for LHC and HHC, Table S4a). Nevertheless, periods of low *water flows* ($Q_i < 800 \text{ m}^3/\text{s}$) mostly
2 3 286 exhibited a transfer driven by tidal-dominated processes and periods of high *water flows* ($800 < Q_i < 2\,000 \text{ m}^3/\text{s}$)
4 5 287 an intermediate behavior considering the high variability both in the *net travelled distances* and the effects of tides
6 7 288 (Table S4a). Resulting from the wide range of *water flow* in the Loire estuary, the shift between tidal-dominated
8 9 289 and river flow-dominated processes therefore appeared gradual. Moreover, by driving macroplastic transfer
10 11 290 distances, hydrological conditions regulate the distance between debris sources and accumulation zones (Duncan
12 13 291 et al., 2020; Tramoy et al., 2020b). It is also interesting to note that in the Loire estuary, more *stranding episodes*
14 15 292 occurred on islands during flood events and HHC (Table S3), because of their submersion. In these cases, the
16 17 293 vegetation on islands constitute strong accumulations zones (Liro et al., 2022). For example, during two
18 19 294 trajectories (T6 and T12), bottles stranded on the uninhabited and therefore highly vegetated La Motte island
20 21 295 (Figure 4). High amount of macrodebris are actually accumulated there, which supports the transfer dynamics
22 23 296 described by the tracked bottles. Furthermore, many authors observed an increase of macroplastics with increasing
24 25 297 *water flows* (Castro-Jiménez et al., 2019; Cheung et al., 2016; Krelling and Turra, 2019; Kurniawan and Imron,
26 27 298 2019b). These trends can result from increasing inputs by the washup from rainwaters on land and/or from the
28 29 299 remobilization of macroplastics accumulated in the river and/or riverbanks (Castro-Jiménez et al., 2019;
30 31 300 Kurniawan and Imron, 2019b; van Emmerik et al., 2022). In the Loire estuary, the percentage of *remobilization*
32 33 301 *episodes* was slightly higher during LHC but the remobilization appeared more efficient (i.e. to cause a subsequent
34 35 302 transfer in the river channel) during HHC (section 3.2). Therefore, the opportunity of the stranded bottles to be
36 37 303 remobilized not only depends on *water flow* but this parameter drives the capacity of the remobilization processes
38 39 304 to be efficient.
40 41 42

43 305 4.1.3. Specific transfer and accumulation processes according to buoyancy

44 306 Macroplastics can be transferred in different ways: floating at the water surface, half-submerged in the
45 46 307 water column or by saltation on the riverbed (van Emmerik et al., 2020a). In the Loire estuary, floating debris
47 48 308 appeared to strand more quickly than half-submerged ones. This behavior was already noticed (Ryan and Perold,
49 50 309 2021; Tramoy et al., 2020b) and one assumption is a greater effect of the wind on debris transferred at the water
51 52 310 surface (Browne et al., 2010; Maclean et al., 2021; van Emmerik and Schwarz, 2020). This is supported in the
53 54 311 Loire estuary by higher *maximum speeds* of floating bottles than half-submerged ones (Table S4b). No correlation
55 56 312 was observed with wind conditions but these variables are difficult to consider because of very local conditions
57 58 313 (e.g. wind gusts). Floating debris will consequently accumulate faster and closer to their entry point in the estuary
59 60 61 62 63 64 65

314 (Maclean et al., 2021), as supported by their low *net distances* (Table S4b). In contrast, half-submerged bottles
1
2 315 appeared more sensitive to the water current than floating bottles and can be longer transported in the water
3
4 316 column. However, like demonstrated by their *net distances*, they travelled not necessarily higher distances by being
5
6 317 more prone to back and forth movements with tides (Figure 3 and 5b, Table S4b). Given these dissimilarities and
7
8 318 based on our feedback on the Loire estuary, buoyancy also affects the storage/remobilization processes. Floating
9
10 319 bottles mostly stranded in intertidal areas whereas half-submerged bottles can be deposited farther from the river
11
12 320 channel (Table S3). Moreover, floating bottles appeared less sensitive to remobilization processes (section 3.3.)
13
14 321 suggesting a higher residence time than half-submerged ones once stranded. Nevertheless, half-submerged bottles
15
16 322 were not always removed until the river channel to be reexported. On the contrary, in some cases (34%), these
17
18 323 *remobilization episodes* pushed them farther from the main channel thanks to the estuarine geomorphology
19
20 324 (submersible areas, plateaux at low elevation, etc.) during high *tidal ranges* (higher than 4 m, Table S2). Two
21
22 325 trajectories actually illustrated this lateral displacement in submersible areas (T7 and T22, Table S3) and the
23
24 326 farthest bottle was retrieved at 1.8 km from the main channel (Figure 4).
25
26
27 327
28

29 328 **4.2. Similarities and specificities with the Seine estuary**

30 329 4.2.1. Macrotidal estuaries as accumulation zone and slow pathway for macroplastics

31
32 330 The same methodology was used in the Seine estuary by Tramoy et al. (2020b). Whatever the estuary
33
34 331 geomorphology (highly and slightly meandered for the Seine and the Loire estuaries, respectively), both surveys
35
36 332 demonstrated chaotic transfer dynamics animated by back and forth movements of the tracked bottles and by
37
38 333 storage/remobilization processes. As demonstrated by Tramoy et al. (2020a, b), these factors increase the residence
39
40 334 time of macroplastics which can tremendously delay their transfer to the ocean. That rivers act as “plastic
41
42 335 reservoirs” was recently conceptualized (Tramoy et al., 2020a; van Emmerik et al., 2022) and a macroplastic
43
44 336 accumulation was also noticed in deltaic systems (Acha et al., 2003; Duncan et al., 2020). Ryan and Perold (2021)
45
46 337 already evoked site-specific transfer distances of macroplastics, mostly resulting from the variable impact of floods
47
48 338 and tides in estuaries. Such processes are therefore not specific but appear enhanced in macrotidal estuaries
49
50 339 considering their water flow-tides relation and their spring and neap tidal cycles. Only 40% of tracked bottles
51
52 340 actually stranded in the Ganga delta (Duncan et al., 2020) whereas no bottles reached the sea during the monitoring
53
54 341 period neither for the Loire nor the Seine estuaries. In the Seine estuary, Tramoy et al. (2020a) estimated a potential
55
56 342 residence time up to decades. In the Loire one, the residence time could not be estimated but is in any case longer
57
58
59
60
61
62
63
64
65

343 than two months. It strengthens the recent suggestion that macrotidal estuarine systems under temperate climates
1 344 mainly act as accumulation zones and slow pathways for macroplastics and that model estimations calculating the
2 345 rates of plastic debris released into the oceans must consider this point (Dris et al., 2020; Tramoy et al., 2020b). It
3 346 also highlights the need to focus on extreme hydrometeorological events, which are most likely to remobilize the
4 347 accumulated macrodebris (van Emmerik et al., 2022).
5
6
7
8
9

10 348 4.2.2. Site-specific dynamics according to estuarine geomorphology

11
12 349 Tracked bottles exhibit different trajectories in both estuaries. Experimental conditions were also variable.
13
14 350 More trajectories were actually monitored during periods of high flows (HHC and floods, n=26) compared to low
15 351 flows (LHC, n=13) in the Seine estuary (Tramoy et al., 2020b) and similar proportions of trajectories were
16 352 monitored during the other hydrological conditions (LHC, n=17 and HHC and floods, n=18) in the Loire one. For
17 353 a better comparison between both estuaries, trajectory parameters were therefore compared for each period (Figure
18 354 6). Regarding bottle's *buoyancy*, experimental conditions were less variable. Similar proportions of half-
19 355 submerged bottles were actually released during periods of high flows (HHC and floods) in both estuaries (56%
20 356 in the Loire estuary, 54% in the Seine one) and quite more in the Loire estuary (53%) than in the Seine one (39%)
21 357 during LHC. The Loire estuary is shorter (i.e. 97 km), lowly meandered (sinuosity index of 1.1), and with higher
22 358 *water flows* (mean $Q_i = 850 \text{ m}^3/\text{s}$) than the Seine one (i.e. 175 km, sinuosity index of 1.9 and mean $Q_i = 487 \text{ m}^3/\text{s}$;
23 359 Tramoy et al., 2020b) offering a better opportunity for macroplastics to be transferred downstream. Despite a
24 360 monitoring on similar time scales, the *travel time in water* was however higher in the Seine estuary than in the
25 361 Loire one whatever the hydrological conditions (Figure 6, Table S5). It leads to *total and net distances* travelled
26 362 by the tracked bottles mostly higher in the Seine estuary than in the Loire one even when compared in relation to
27 363 the total estuarine length (Figure 6, Table S5). Therefore, even if meanders are known to enable a greater
28 364 macroplastic accumulation than linear river sections (Mazarrasa et al., 2019; van Emmerik et al., 2019), the higher
29 365 meandering morphology of the Seine estuary (Tramoy et al., 2020b) does not necessarily mean a quick stranding
30 366 of macroplastics, or at least a high residence time once stranded. In fact, the trajectories recorded in the Seine
31 367 estuary exhibited a higher number of *stranding episodes* than the Loire one (Figure 6, Table S5), suggesting that
32 368 remobilization processes occur easily and more frequently. These different dynamics can be related to the
33 369 difference of riverbank typologies between both estuaries. Liro et al. (2020) actually hypothesized that rivers with
34 370 more diverse morphologies (wider channel, floodplain zones, islands and lateral channels) and riparian vegetations
35 371 (case of the Loire River) could limit the downstream transport of macroplastics compared to channelized and
36 372 embanked rivers (case of the Seine River). Results of this study illustrate this hypothesis and confirm that the
37
38
39
40
41
42
43
44
45
46
47
48
49
50
51
52
53
54
55
56
57
58
59
60
61
62
63
64
65

373 geomorphology of the Loire estuary limit the transfer of the tracked bottles which are accumulated in areas where
1
2 374 they are difficult to remove (submersible areas, islands, lateral channels, etc.).
3

4 375 4.2.3. Site-specific accumulation zones according to estuarine geomorphology 5 6

7 376 Estuarine geomorphology is a predominant factor for creating macroplastic accumulation areas. Firstly,
8
9 377 features like riverbanks with gentle slope (Browne et al., 2010; Bruge et al., 2018; Cordeiro and Costa, 2010),
10
11 378 meanders (Mazarrasa et al., 2019; Tramoy et al., 2020b) or high and flat areas (Ivar do Sul et al., 2014) were
12
13 379 recognized as preferential areas for accumulating macroplastics. The gentle slope as well as the presence of islands
14
15 380 and large submersible areas tend to favor the macroplastics retention in the Loire estuary, whereas the Seine natural
16
17 381 riverbanks are steeper. Secondly, large riparian vegetation also constitutes great accumulation zones according to
18
19 382 literature (e.g. Bruge et al., 2018; Gonçalves et al., 2020; Ivar do Sul et al., 2014; Weideman et al., 2020; Williams
20
21 383 and Simmons, 1997) and the Loire estuary is no exception. The trapping capacity of vegetation is driven by its
22
23 384 structural characteristics (Mazarrasa et al., 2019) such as their height, plant density and spatial configuration (van
24
25 385 Emmerik et al., 2022). A significant retention capacity for reedbeds has already been suggested (van Emmerik and
26
27 386 Schwarz, 2020). The great storage of macroplastics in reedbeds in the downstream part of the Loire estuary (Figure
28
29 387 4; GIP, 2016) confirm this suggestion. This is also demonstrated by the low proportions of *remobilization episodes*
30
31 388 for the bottles stranded in this type of riparian vegetation (Figure 4, Table S3). The short length of the Loire estuary
32
33 389 actually enables the macroplastics to reach faster these strong accumulation zones. Accumulation zones can
34
35 390 therefore show a large variability according to the estuaries considered (Rech et al., 2014). Most of the time,
36
37 391 accumulation zones are very localized (Ryan and Perold, 2021) and site-specific investigations thus provide useful
38
39 392 insights to locally optimize plastic recovery strategies (van Calcar and van Emmerik, 2019). In the Seine estuary
40
41 393 for example, the Villequier site is known to strongly accumulate macroplastics and is regularly cleaned up as well
42
43 394 as other accumulation zones (Tramoy et al., 2021). In the Loire estuary, accumulation zones appeared more diverse
44
45 395 but some areas downstream from Nantes agglomeration and reedbeds were identified as significant ones (Figure
46
47 396 4). Regular clean up actions similarly to those realized in the Seine estuary could therefore be planned. If not, it
48
49 397 can either be supposed that seasonal changes in the riparian vegetation may provoke the release of the accumulated
50
51 398 debris or that these may be degraded into microplastics (Dris et al., 2020; Gonçalves et al., 2020; Ivar do Sul et
52
53 399 al., 2014) creating a source of secondary microplastic within the riverine and marine ecosystems.
54
55
56
57 400
58
59

60 401 5. Concluding remarks, outlooks and recommendations 61 62 63 64 65

402 Macroplastic transfer dynamics show a high spatiotemporal variability within estuaries making it difficult
1
2 403 to qualify, quantify and therefore to predict. Nevertheless, we have to improve our understanding of macroplastics
3
4 404 evolution for a better management of this contamination and this study provides valuable information on their
5
6 405 transfer and accumulation dynamics within an estuary at short temporal scale. Consistently with other studies on
7
8 406 estuaries, this study illustrates that tides lead to chaotic and stepwise macroplastic transfer dynamics animated by
9
10 407 back and forth movements and storage/remobilization processes. Such processes appear not specific but enhanced
11
12 408 in macrotidal estuaries where tidal ranges are the highest. On the 74 tracked bottles released either in the Seine or
13
14 409 in the Loire estuaries, none reached the ocean during their active tracking (up to two months), suggesting estuaries
15
16 410 constitute slow pathways or even a long-lasting macroplastic reservoir. Those results raise questions about the real
17
18 411 amount of macroplastics entering into the ocean when compared to model estimations. The enhanced downstream
19
20 412 transport under flooding conditions balanced by enhanced storage/remobilization processes also highlights the key
21
22 413 role of extreme events like flood events, all the more so with the ongoing climate change.

23
24
25 414 This study also corroborates that macroplastic buoyancy significantly influences their transfer dynamics
26
27 415 and therefore their accumulation zones and residence time whatever the type of estuary considered. However,
28
29 416 whatever their buoyancy, the macroplastic transport in macrotidal estuaries may be tidal-dominated under regular
30
31 417 hydrological conditions, whereas it may be driven by river flow-dominated processes during high water discharge
32
33 418 (i.e. flood events) strengthening again the need to focus on extreme hydrometeorological events. These trends
34
35 419 appear however valid for macrotidal estuaries under temperate climates but more studies are required to confirm
36
37 420 this hypothesis. The latter carried with comparable data and on different type of estuaries could be highly valuable.
38
39 421 By choosing a stochastic approach to observe macroplastic transfer dynamics, we assume that only general trends
40
41 422 can be concluded from the results. A precise assessment of the influence of tidal range, water flows and the
42
43 423 different parts of the estuary (estuarine-fluviale zone, internal and external parts) requires a deterministic approach
44
45 424 in the sample design like it was done for bottle's buoyancy. Nevertheless, the consideration of such variables needs
46
47 425 a careful thought as their spatiotemporal variability are difficult to integrate. For example, the clustering designed
48
49 426 relative to the water flow considered the water flow at start time and do not include all variations during
50
51 427 trajectories. The difficulty is the same to evaluate the influence of wind gusts on floating macroplastic dynamics.

52
53
54 428 Moreover, intertidal areas and riparian vegetations are major actors of macroplastic retention and large
55
56 429 accumulation zones have been identified in both estuaries. Nevertheless, given the specific geomorphology of the
57
58 430 Loire estuary with large submersible areas, the presence of reedbeds, islands and lateral channels, it appears as a
59
60 431 more efficient sink for macroplastics than the Seine one. Accumulation zones were actually more diverse and
61
62
63
64
65

432 widely distributed, sometimes far from the river channel. Such site-specific studies provide also important
1
2 433 information for a better adaptation of our macroplastic removal strategies. Among the accumulation zones
3
4 434 identified through this work, some will be subject to a monitoring while cleaning actions are already led on some
5
6 435 others.

7
8
9 436

11 437 **Acknowledgments**

14 438 This work, was funded by Région des Pays de la Loire (France) and by Nantes Métropole within the framework
15
16 439 of the Plasti-nium Research project. This project benefit from the scientific structuration of the Sciences of the
17
18 440 Universe Observatory of Nantes (OSUNA) and its program “Grande Zone Estuarienne et Risques” (GZER). The
19
20 441 authors gratefully thank the GIP Loire Estuaire for providing geographical data layer on the Loire estuary.

21
22
23 442

26 443 **References**

- 28 444 Acha, E.M., Mianzan, H.W., Iribarne, O., Gagliardini, D.A., Lasta, C., Daleo, P., 2003. The role of the Río de la Plata bottom
29 445 salinity front in accumulating debris. *Marine Pollution Bulletin* 46, 197–202. [https://doi.org/10.1016/S0025-](https://doi.org/10.1016/S0025-326X(02)00356-9)
30 446 [326X\(02\)00356-9](https://doi.org/10.1016/S0025-326X(02)00356-9)
- 31 447 Biermann, L., Clewley, D., Martinez-Vicente, V., Topouzelis, K., 2020. Finding Plastic Patches in Coastal Waters using Optical
32 448 Satellite Data. *Scientific Reports* 10, 5364. <https://doi.org/10.1038/s41598-020-62298-z>
- 33 449 Boët, P., Bocquené, G., Bouleau, G., Etchebert, H., Foussard, V., Just, A., Lepage, M., Lobry, J., Moussard, S., Sirost, O.,
34 450 Sottolichio, A., Leveque, C., 2011. Synthèse du projet BEEST. Rapport de l'IRSTEA.
- 35 451 Briant, N., Chiffolleau, J.-F., Knoery, J., Araújo, D.F., Ponzevera, E., Crochet, S., Thomas, B., Brach-Papa, C., 2021. Seasonal
36 452 trace metal distribution, partition and fluxes in the temperate macrotidal Loire Estuary (France). *Estuarine, Coastal
37 453 and Shelf Science* 262, 107616. <https://doi.org/10.1016/j.ecss.2021.107616>
- 38 454 Browne, M.A., Galloway, T.S., Thompson, R.C., 2010. Spatial Patterns of Plastic Debris along Estuarine Shorelines.
39 455 *Environmental Science & Technology* 44, 3404–3409. <https://doi.org/10.1021/es903784e>
- 40 456 Bruge, A., Barreau, C., Carlot, J., Collin, H., Moreno, C., Maison, P., 2018. Monitoring Litter Inputs from the Adour River
41 457 (Southwest France) to the Marine Environment. *Journal of Marine Science and Engineering* 6, 24.
42 458 <https://doi.org/10.3390/jmse6010024>
- 43 459 Castro-Jiménez, J., González-Fernández, D., Fornier, M., Schmidt, N., Sempéré, R., 2019. Macro-litter in surface waters from
44 460 the Rhone River: Plastic pollution and loading to the NW Mediterranean Sea. *Marine Pollution Bulletin* 146, 60–66.
45 461 <https://doi.org/10.1016/j.marpolbul.2019.05.067>
- 46 462 Cheung, P.K., Cheung, L.T.O., Fok, L., 2016. Seasonal variation in the abundance of marine plastic debris in the estuary of a
47 463 subtropical macro-scale drainage basin in South China. *Science of The Total Environment* 562, 658–665.
48 464 <https://doi.org/10.1016/j.scitotenv.2016.04.048>
- 49 465 Cordeiro, C.A.M.M., Costa, T.M., 2010. Evaluation of solid residues removed from a mangrove swamp in the São Vicente
50 466 Estuary, SP, Brazil. *Marine Pollution Bulletin* 60, 1762–1767. <https://doi.org/10.1016/j.marpolbul.2010.06.010>
- 51 467 Dris, R., Tramoy, R., Alligant, S., Gasperi, J., Tassin, B., 2020. Plastic Debris Flowing from Rivers to Oceans: The Role of the
52 468 Estuaries as a Complex and Poorly Understood Key Interface, in: Rocha-Santos, T., Costa, M., Mouneyrac, C. (Eds.),
53 469 *Handbook of Microplastics in the Environment*. Springer International Publishing, Cham, pp. 1–28.
54 470 https://doi.org/10.1007/978-3-030-10618-8_3-1
- 55 471 Duncan, E.M., Davies, A., Brooks, A., Chowdhury, G.W., Godley, B.J., Jambeck, J., Maddalene, T., Napper, I., Nelms, S.E.,
56 472 Rackstraw, C., Koldewey, H., 2020. Message in a bottle: Open source technology to track the movement of plastic
57 473 pollution. *PLoS ONE* 15, e0242459. <https://doi.org/10.1371/journal.pone.0242459>
- 58 474 GIP, 2014. Les mouvements. Les sédiments. La dynamique du bouchon vaseux. Cahier indicateur du GIP Loire Estuaire 1.
59 475 GIP, 2016. Inventaire des roselières de l'estuaire de la Loire, acquisition et analyse de données. Précisions méthodologiques et
60 476 analyse diachronique. Rapport du GIP Loire Estuaire.

477 Gonçalves, M., Schmid, K., Andrade, M.C., Andrades, R., Pegado, T., Giarrizzo, T., 2020. Are the tidal flooded forests sinks
478 for litter in the Amazonian estuary? *Marine Pollution Bulletin* 161, 111732.
479 <https://doi.org/10.1016/j.marpolbul.2020.111732>

480 González-Fernández, D., Cózar, A., Hanke, G., Viejo, J., Morales-Caselles, C., Bakiu, R., Barceló, D., Bessa, F., Bruge, A.,
481 Cabrera, M., Castro-Jiménez, J., Constant, M., Crosti, R., Galletti, Y., Kideys, A.E., Machitadze, N., Pereira de Brito,
482 J., Pogojeva, M., Ratola, N., Rigueira, J., Rojo-Nieto, E., Savenko, O., Schöneich-Argent, R.I., Siedlewicz, G.,
483 Suaria, G., Tourgeli, M., 2021. Floating macrolitter leaked from Europe into the ocean. *Nature Sustainability* 4, 474–
484 483. <https://doi.org/10.1038/s41893-021-00722-6>

485 Hajbane, S., Pattiaratchi, C.B., 2017. Plastic Pollution Patterns in Offshore, Nearshore and Estuarine Waters: A Case Study
486 from Perth, Western Australia. *Frontiers in Marine Science* 4. <https://doi.org/10.3389/fmars.2017.00063>

487 Ivar do Sul, J.A., Costa, M.F., 2013. Plastic pollution risks in an estuarine conservation unit. *Journal of Coastal Research* 65,
488 48–53. <https://doi.org/10.2112/SI65-009.1>

489 Ivar do Sul, J.A., Costa, M.F., Silva-Cavalcanti, J.S., Araújo, M.C.B., 2014. Plastic debris retention and exportation by a
490 mangrove forest patch. *Marine Pollution Bulletin* 78, 252–257. <https://doi.org/10.1016/j.marpolbul.2013.11.011>

491 Kassambara, A., Mundt, F., 2020. Factoextra: Extract and Visualize the Results of Multivariate Data Analyses. R Package
492 Version 1.0.7. <https://CRAN.R-project.org/package=factoextra>

493 Krelling, A.P., Turra, A., 2019. Influence of oceanographic and meteorological events on the quantity and quality of marine
494 debris along an estuarine gradient. *Marine Pollution Bulletin* 139, 282–298.
495 <https://doi.org/10.1016/j.marpolbul.2018.12.049>

496 Kurniawan, S.B., Imron, M.F., 2019a. The effect of tidal fluctuation on the accumulation of plastic debris in the Wonorejo
497 River Estuary, Surabaya, Indonesia. *Environmental Technology & Innovation* 15, 100420.
498 <https://doi.org/10.1016/j.eti.2019.100420>

499 Kurniawan, S.B., Imron, M.F., 2019b. Seasonal variation of plastic debris accumulation in the estuary of Wonorejo River,
500 Surabaya, Indonesia. *Environmental Technology & Innovation* 16, 100490.
501 <https://doi.org/10.1016/j.eti.2019.100490>

502 Lê, S., Josse, J., Husson, F., 2008. FactoMineR: An R Package for Multivariate Analysis. *Journal of Statistical Software* 25.
503 <https://doi.org/10.18637/jss.v025.i01>

504 Lechthaler, S., Waldschläger, K., Stauch, G., Schüttrumpf, H., 2020. The Way of Macroplastic through the Environment.
505 *Environments* 7, 73. <https://doi.org/10.3390/environments7100073>

506 Liro, M., Emmerik, T. van, Wyzga, B., Liro, J., Mikuś, P., 2020. Macroplastic Storage and Remobilization in Rivers. *Water*
507 12, 2055. <https://doi.org/10.3390/w12072055>

508 Liro, M., Mikuś, P., Wyzga, B., 2022. First insight into the macroplastic storage in a mountain river: The role of in-river
509 vegetation cover, wood jams and channel morphology. *Science of The Total Environment* 838, 156354.
510 <https://doi.org/10.1016/j.scitotenv.2022.156354>

511 Maclean, K., Weideman, E.A., Perold, V., Ryan, P.G., 2021. Buoyancy affects stranding rate and dispersal distance of floating
512 litter entering the sea from river mouths. *Marine Pollution Bulletin* 173, 113028.
513 <https://doi.org/10.1016/j.marpolbul.2021.113028>

514 Maximenko, N., Corradi, P., Law, K.L., Van Sebille, E., Garaba, S.P., Lampitt, R.S., Galgani, F., Martinez-Vicente, V.,
515 Goddijn-Murphy, L., Veiga, J.M., Thompson, R.C., Maes, C., Moller, D., Löscher, C.R., Addamo, A.M., Lamson,
516 M.R., Centurioni, L.R., Posth, N.R., Lumpkin, R., Vinci, M., Martins, A.M., Pieper, C.D., Isobe, A., Hanke, G.,
517 Edwards, M., Chubarenko, I.P., Rodriguez, E., Aliani, S., Arias, M., Asner, G.P., Brosich, A., Carlton, J.T., Chao,
518 Y., Cook, A.-M., Cundy, A.B., Galloway, T.S., Giorgetti, A., Goni, G.J., Guichoux, Y., Haram, L.E., Hardesty, B.D.,
519 Holdsworth, N., Lebreton, L., Leslie, H.A., Macadam-Somer, I., Mace, T., Manuel, M., Marsh, R., Martinez, E.,
520 Mayor, D.J., Le Moigne, M., Molina Jack, M.E., Mowlem, M.C., Obbard, R.W., Pabortsava, K., Robberson, B.,
521 Rotaru, A.-E., Ruiz, G.M., Spedicato, M.T., Thiel, M., Turra, A., Wilcox, C., 2019. Toward the Integrated Marine
522 Debris Observing System. *Frontiers in Marine Science* 6, 447. <https://doi.org/10.3389/fmars.2019.00447>

523 Mazarrasa, I., Puente, A., Núñez, P., García, A., Abascal, A.J., Juanes, J.A., 2019. Assessing the risk of marine litter
524 accumulation in estuarine habitats. *Marine Pollution Bulletin* 144, 117–128.
525 <https://doi.org/10.1016/j.marpolbul.2019.04.060>

526 Meijer, L.J.J., van Emmerik, T., van der Ent, R., Schmidt, C., Lebreton, L., 2021. More than 1000 rivers account for 80% of
527 global riverine plastic emissions into the ocean. *Science Advances* 7, eaaz5803.
528 <https://doi.org/10.1126/sciadv.aaz5803>

529 Pinheiro, L.M., Agostini, V.O., Lima, A.R.A., Ward, R.D., Pinho, G.L.L., 2021. The fate of plastic litter within estuarine
530 compartments: An overview of current knowledge for the transboundary issue to guide future assessments.
531 *Environmental Pollution* 279, 116908. <https://doi.org/10.1016/j.envpol.2021.116908>

532 Possatto, F.E., Spach, H.L., Cattani, A.P., Lamour, M.R., Santos, L.O., Cordeiro, N.M.A., Broadhurst, M.K., 2015. Marine
533 debris in a World Heritage Listed Brazilian estuary. *Marine Pollution Bulletin* 91, 548–553.
534 <https://doi.org/10.1016/j.marpolbul.2014.09.032>

535 QGIS.org, 2022. QGIS Geographic Information System. QGIS Association. <http://www.qgis.org>

536 Rech, S., Macaya-Caquilpán, V., Pantoja, J.F., Rivadeneira, M.M., Jofre Madariaga, D., Thiel, M., 2014. Rivers as a source of
537 marine litter – A study from the SE Pacific. *Marine Pollution Bulletin* 82, 66–75.
538 <https://doi.org/10.1016/j.marpolbul.2014.03.019>

539 RStudio Team, 2021. RStudio: Integrated Development Environment for R. RStudio, PBC, Boston, MA.
540 <http://www.rstudio.com/>

541 Ryan, P.G., Perold, V., 2021. Limited dispersal of riverine litter onto nearby beaches during rainfall events. *Estuarine, Coastal
542 and Shelf Science* 251, 107186. <https://doi.org/10.1016/j.ecss.2021.107186>

543 Sadri, S.S., Thompson, R.C., 2014. On the quantity and composition of floating plastic debris entering and leaving the Tamar
544 Estuary, Southwest England. *Marine Pollution Bulletin* 81, 55–60. <https://doi.org/10.1016/j.marpolbul.2014.02.020>
1 545 SAGE, 2020. Plan d'aménagement et de gestion durable de la ressource en eau. Rapport du Schéma d'aménagement et de
2 546 gestion des eaux, Estuaire de la Loire.
3 547 Schmidt, C., Krauth, T., Wagner, S., 2017. Export of Plastic Debris by Rivers into the Sea. *Environmental Science &*
4 548 *Technology* 51, 12246–12253. <https://doi.org/10.1021/acs.est.7b02368>
5 549 Schöneich-Argent, R.I., Dau, K., Freund, H., 2020. Wasting the North Sea? – A field-based assessment of anthropogenic
6 550 macrolitter loads and emission rates of three German tributaries. *Environmental Pollution* 263, 114367.
7 551 <https://doi.org/10.1016/j.envpol.2020.114367>
8 552 Sellier, D., 2012. Géomorphologie de l'estuaire de la Loire, éléments de vulgarisation et de patrimonialisation. *Cahiers Nantais*
9 553 *d'Aménagement* 1, 45–64.
10 554 SNPN, 2008. Estuaires, deltas et baies. Rapport de la Société nationale de protection de la nature. *Zones Humides Infos* 61, 32.
11 555 Tramoy, R., Gasperi, J., Colasse, L., Tassin, B., 2020a. Transfer dynamic of macroplastics in estuaries — New insights from
12 556 the Seine estuary: Part 1. Long term dynamic based on date-prints on stranded debris. *Marine Pollution Bulletin* 152,
13 557 110894. <https://doi.org/10.1016/j.marpolbul.2020.110894>
14 558 Tramoy, R., Gasperi, J., Colasse, L., Silvestre, M., Dubois, P., Noûs, C., Tassin, B., 2020b. Transfer dynamics of macroplastics
15 559 in estuaries – New insights from the Seine estuary: Part 2. Short-term dynamics based on GPS-trackers. *Marine*
16 560 *Pollution Bulletin* 160, 111566. <https://doi.org/10.1016/j.marpolbul.2020.111566>
17 561 Tramoy, R., Gasperi, J., Colasse, L., Noûs, C., Tassin, B., 2021. Transfer dynamics of macroplastics in estuaries – New insights
18 562 from the Seine estuary: Part 3. What fate for macroplastics? *Marine Pollution Bulletin* 169, 112513.
19 563 <https://doi.org/10.1016/j.marpolbul.2021.112513>
20 564 van Calcar, C.J., van Emmerik, T.H.M., 2019. Abundance of plastic debris across European and Asian rivers. *Environmental*
21 565 *Research Letters* 14, 124051. <https://doi.org/10.1088/1748-9326/ab5468>
22 566 van Emmerik, T., Strady, E., Kieu-Le, T.-C., Nguyen, L., Gratiot, N., 2019. Seasonality of riverine macroplastic transport. *Sci*
23 567 *Rep* 9, 13549. <https://doi.org/10.1038/s41598-019-50096-1>
24 568 van Emmerik, T., Schwarz, A., 2020. Plastic debris in rivers. *WIREs Water* 7, e1398. <https://doi.org/10.1002/wat2.1398>
25 569 van Emmerik, T., Roebroek, C., de Winter, W., Vriend, P., Boonstra, M., Hougee, M., 2020a. Riverbank macrolitter in the
26 570 Dutch Rhine–Meuse delta. *Environmental Research Letters* 15, 104087. <https://doi.org/10.1088/1748-9326/abb2c6>
27 571 van Emmerik, T., van Klaveren, J., Meijer, L.J.J., Krooshof, J.W., Palmos, D.A.A., Tanchuling, M.A., 2020b. Manila River
28 572 Mouths Act as Temporary Sinks for Macroplastic Pollution. *Frontiers in Marine Science* 7, 545812.
29 573 <https://doi.org/10.3389/fmars.2020.545812>
30 574 van Emmerik, T., Mellink, Y., Hauk, R., Waldschläger, K., Schreyers, L., 2022. Rivers as Plastic Reservoirs. *Frontiers in Water*
31 575 3, 786936. <https://doi.org/10.3389/frwa.2021.786936>
32 576 Vegter, A., Barletta, M., Beck, C., Borrero, J., Burton, H., Campbell, M., Costa, M., Eriksen, M., Eriksson, C., Estrades, A.,
33 577 Gilardi, K., Hardesty, B., Ivar do Sul, J., Lavers, J., Lazar, B., Lebreton, L., Nichols, W., Ribic, C., Ryan, P., Schuyler,
34 578 Q., Smith, S., Takada, H., Townsend, K., Wabnitz, C., Wilcox, C., Young, L., Hamann, M., 2014. Global research
35 579 priorities to mitigate plastic pollution impacts on marine wildlife. *Endangered Species Research* 25, 225–247.
36 580 <https://doi.org/10.3354/esr00623>
37 581 Vermeiren, P., Muñoz, C.C., Ikejima, K., 2016. Sources and sinks of plastic debris in estuaries: A conceptual model integrating
38 582 biological, physical and chemical distribution mechanisms. *Marine Pollution Bulletin* 113, 7–16.
39 583 <https://doi.org/10.1016/j.marpolbul.2016.10.002>
40 584 Weideman, E.A., Perold, V., Arnold, G., Ryan, P.G., 2020. Quantifying changes in litter loads in urban stormwater run-off
41 585 from Cape Town, South Africa, over the last two decades. *Science of The Total Environment* 724, 138310.
42 586 <https://doi.org/10.1016/j.scitotenv.2020.138310>
43 587 Wickham, H., 2016. *ggplot2: Elegant Graphics for Data Analysis*. Springer-Verlag New York. <https://ggplot2.tidyverse.org>
44 588 Williams, A.T., Simmons, S.L., 1997. Movement patterns of riverine litter. *Water, Air, and Soil Pollution* 98, 119–139.
45 589 <https://doi.org/10.1007/BF02128653>
46
47
48
49
50
51
52
53
54
55
56
57
58
59
60
61
62
63
64
65

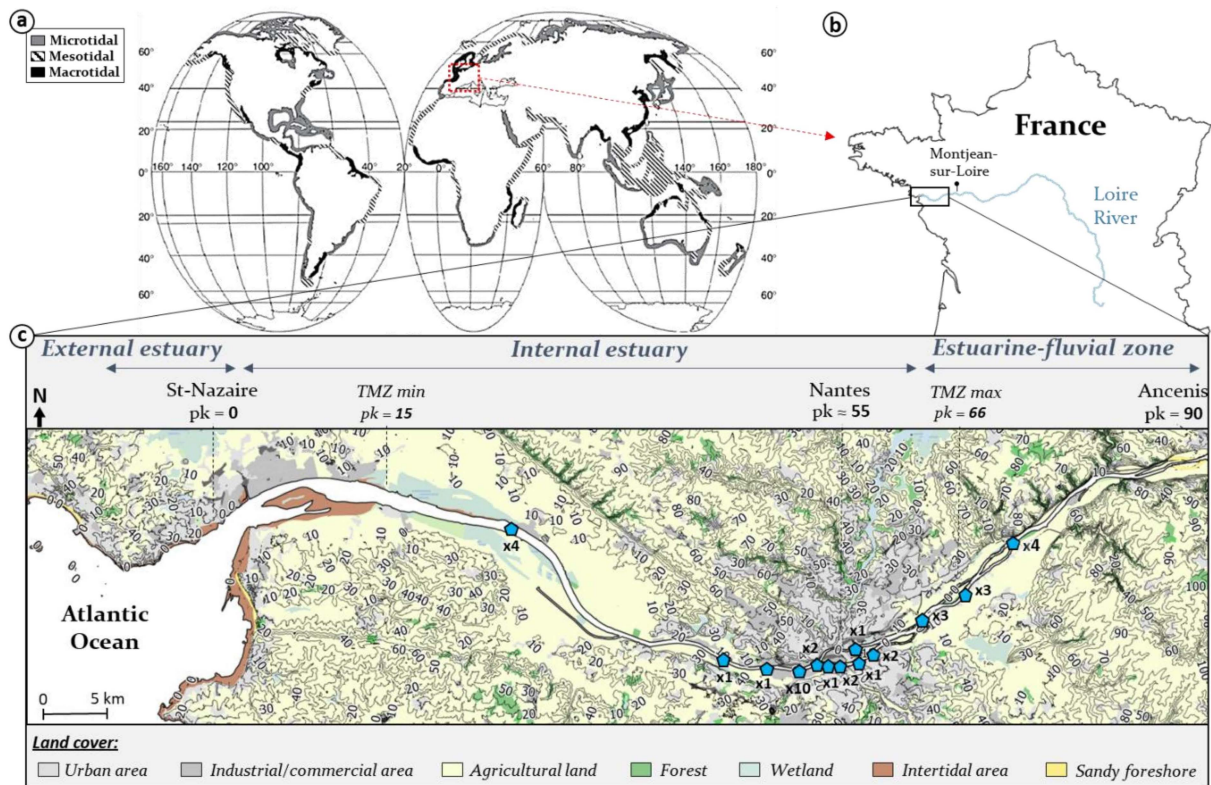
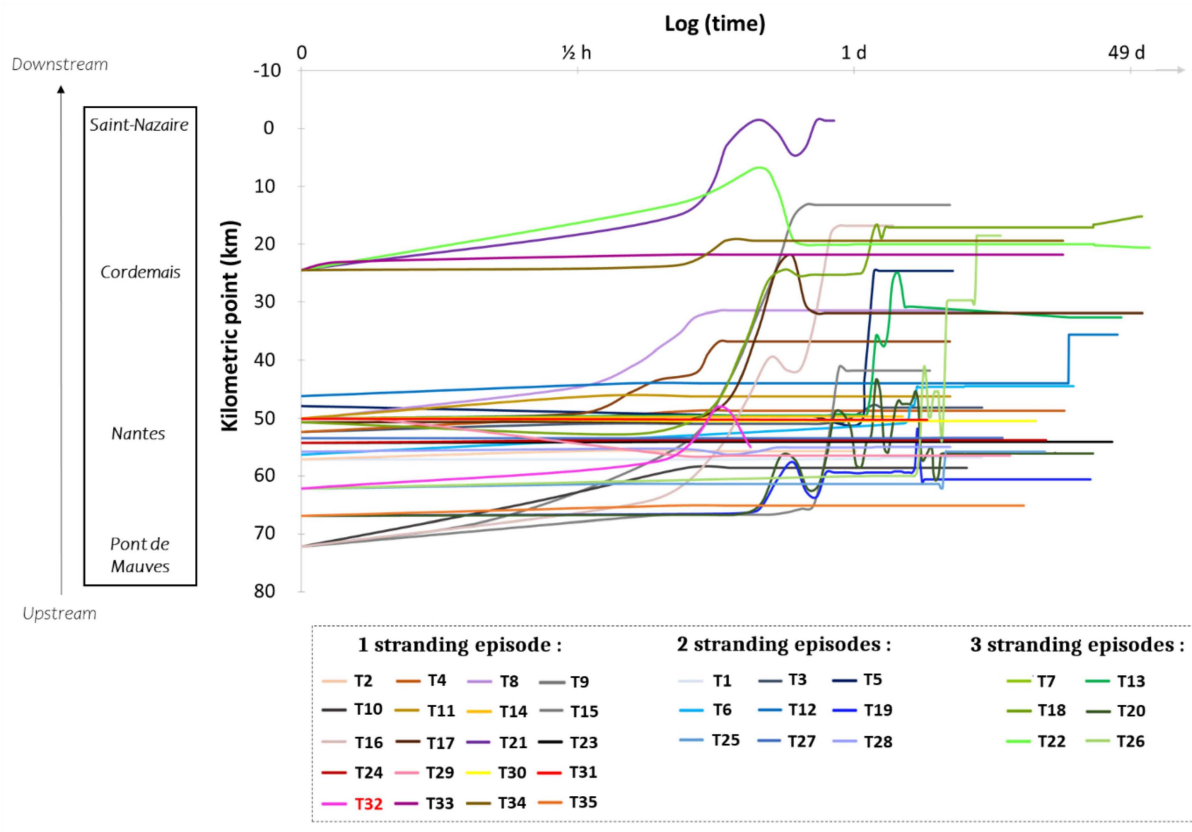


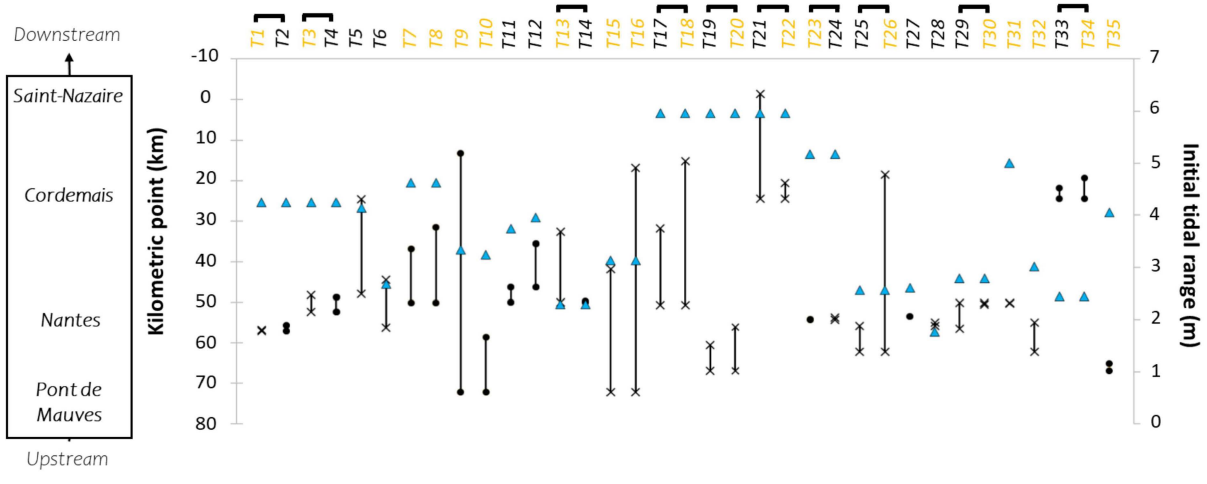
Figure 1: a) World map of the types of estuaries (www.aquaportail.com) and position of France, b) map of France and of the Loire estuary, c) map of the Loire estuary with the tracked bottles sites of release (blue pentagons). The number of tracked bottles released is indicated. The kilometric point (pk) 0 is set in St-Nazaire, pk are positively increasing upstream and negative downstream. From up to downstream, the tracked bottles were released in Mauves-sur-Loire (pk 72.2, Mid-bridge), St-Julien-de-Concelles (pk 66.9, Mid-bridge), Basse-Goulaine (pk 62.2, Mid-bridge), St-Sebastien-sur-Loire (pk 57.1, Mid-bridge), Nantes (pk 56.3 & 55.8, Mid-bridge; pk 50.7, 50.2, 50.1 & 50, Riverbanks), Rezé (pk 54.3, Mid-bridge; pk 53.5 & 52.4, Riverbanks), Bougenais (pk 47.9 & 46.2, Riverbanks) and le Pellerin (pk 24.5, Riverbanks). The land cover (Corine Land Cover 2018 from www.data.gouv.fr), the topography, and the minimum and maximum positions of the Turbidity Maximum Zone (TMZ) are indicated.

1
2
3
4
5
6
7
8
9
10
11
12
13
14
15
16
17
18
19
20
21
22
23
24
25
26
27
28
29
30
31
32
33
34
35
36
37
38
39
40
41
42
43
44
45
46
47
48
49
50
51
52
53
54
55
56
57
58
59
60
61
62
63
64
65



602
603
604
605
606
607

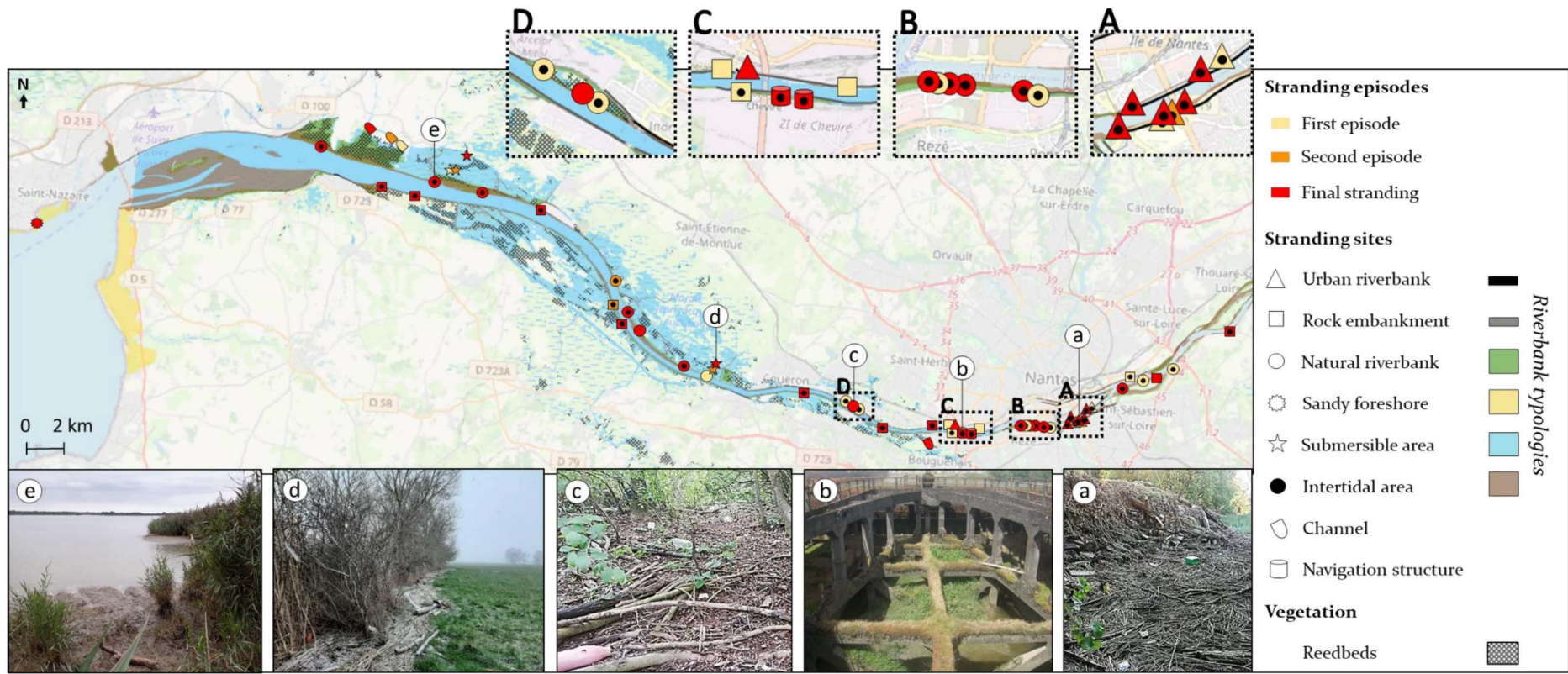
Figure 2: Kilometric point (pk in km) of the tracked bottles according to time (in hours noted h and days noted d) in a logarithmic scale. Colors of the trajectories were set according to the number of stranding episodes: random colors for 1 stranding episode (T32 appears in red since because of the loss of the signal no stranding episode was actually monitored), blue shades for 2 stranding episodes and green shades for 3 stranding episodes.



608
609
610
611
612
613

Figure 3: Net distances (in km) travelled by the tracked bottles from the initial to the final Kilometric point (pk) according to the initial tidal range (blue triangles, in m). The trajectories for which a difference between total and net distances was observed are represented by crosses at initial and final points. Trajectories of floating bottles are named in black, trajectories of half-submerged bottles are named in yellow and paired bottles are indicated by brackets.

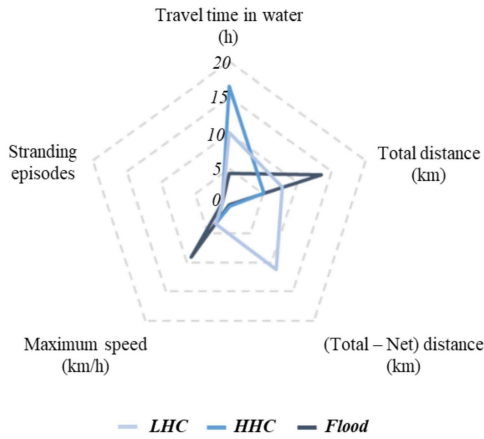
16
17
18
19
20
21
22
23
24
25
26
27
28
29
30
31
32
33
34
35
36
37
38
39
40
41
42
43
44
45
46
47
48
49
50
51
52
53
54
55
56
57
58
59
60
61
62
63
64
65



614

615 *Figure 4: Map of the stranding conditions of the tracked bottles with colors corresponding to their potential remobilization and symbols corresponding to the stranding sites.*
 616 *The riverbank typologies and the presence of reedbeds (data from the GIP Loire Estuaire) in the Loire estuary are represented as well as photos of some accumulation zones*
 617 *(a: at fixed urban riverbanks south of Nantes Métropole, b: in harbor structures, c: at the la Motte island, d: at riparian vegetation of submersible areas, e: in reedbeds).*

a) Hydrological conditions



b) Buoyancy

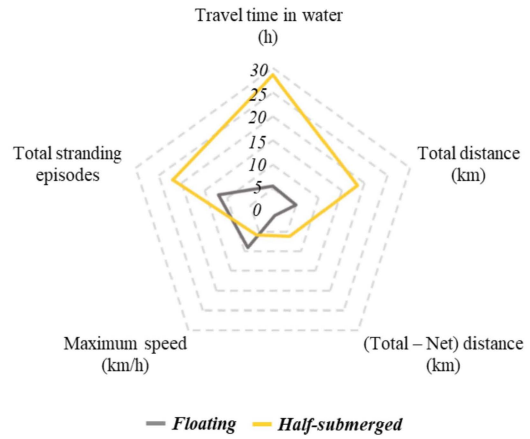


Figure 5: a) Median values of different parameters according to hydrological conditions (Low hydrological conditions, $n(LHC) = 17$; High hydrological conditions, $n(HHC) = 12$; and $n(Flood) = 6$). b) Median values of travel time in water (in hours noted h), total distance and (Total - Net) distance (in km), maximum values of speeds (in km/h) and total number of stranding episodes according to bottles buoyancy (floating, $n = 10$; and half-submerged, $n = 10$).

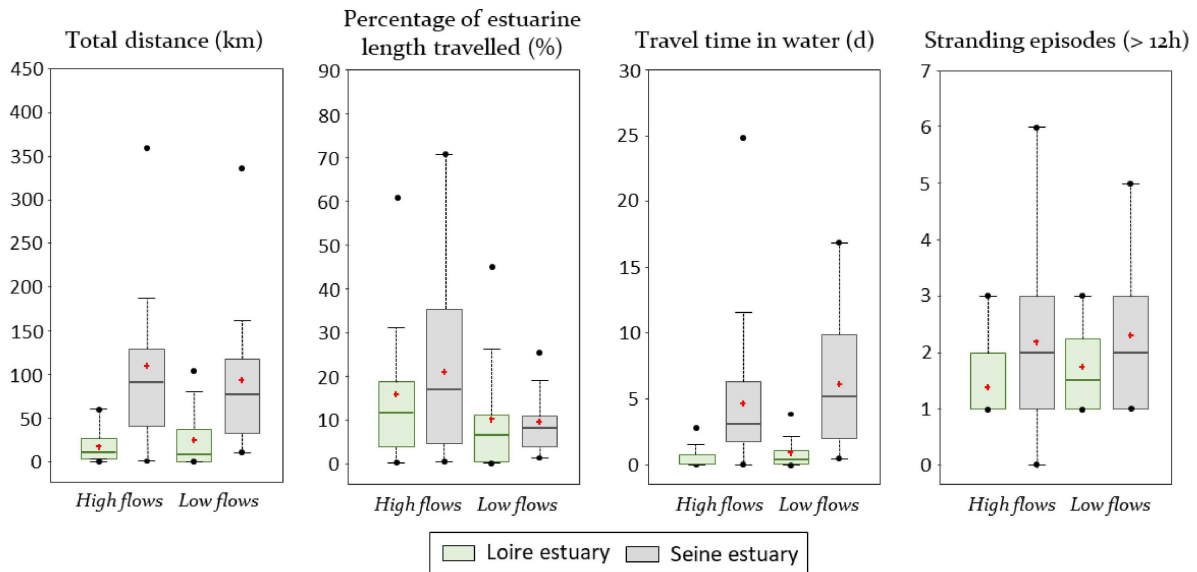


Figure 6: Boxplots representing the variability (first quartile, third quartile and median; red crosses: mean values; vertical bars: 1.5 time the interquartile range) of the total distance (in km), the percentages of estuarine length travelled by the bottles (calculated by dividing the net distance by the total length of estuary), the travel time in water (in days noted d) and the number of stranding episodes according to the estuary considering the hydrological conditions: high ($n(Loire) = 18$; and $n(Seine) = 23$) and low flows ($n(Loire) = 17$; and $n(Seine) = 13$).

632 *Table 1: Parameters describing initial and final conditions, durations, distances, speeds and*
633 *stranding/remobilization conditions of the trajectories in the Loire River. Parameters reporting*
634 *hydrometeorological conditions are also included. All the results of these parameters are reported in the*
635 *supplementary materials. Black stars indicate the common parameters with the study in the Seine estuary (Tramoy*
636 *et al., 2020b).*

Initial conditions		
<i>Start time*</i>	Day and time of release	Date, hour
<i>Site of release*</i>	Geographical site where the tracked bottle was released	-
<i>Start pk*</i>	Kilometric point (pk) of the site of release	Km
<i>Buoyancy*</i>	Buoyancy of the tracked bottle (e.g. floating or half-submerged)	-
Final conditions		
<i>End time*</i>	Day and time of the last GPS position recorded	Date, hour
<i>Last stranding*</i>	Day and time of the last stranding before loss of signal or bottle retrieve	Date, hour
<i>End site*</i>	Geographical site where the tracked bottle was retrieved or lost	-
<i>End pk*</i>	Kilometric point (pk) of the end site	Km
Durations		
<i>Total duration</i>	Time between end time and start time including periods of stranding (> 12h)	Day
<i>Travel Time*</i>	Time between last stranding and start time including periods of stranding (> 12h)	Day
<i>Travel Time in water*</i>	Time between last stranding and start time without periods of stranding (> 12h)	Day
<i>Stranding Time*</i>	Cumulative time of stranding (> 12h) until last stranding	Day
Distances		
<i>Total distance*</i>	Cumulative distance between absolute values of pk of each GPS position	Km
<i>Net distance*</i>	Net distance travelled by the tracked bottles	Km

<i>(Total - Net) distances</i>	Difference between total and net distances travelled by the tracked bottles	Km
Speeds		
<i>Maximum speed</i>	Maximum speed reached by the tracked bottles during their travel time in water	Km/h
Stranding/remobilization conditions		
<i>Stranding episodes (> 12h)*</i>	Number of stranding episodes greater than a complete tidal cycle	-
<i>Remobilization episodes</i>	Number of remobilization episodes	-
<i>Date of stranding</i>	Day and time of stranding	Date, hour
<i>Date of remobilization</i>	Day and time of remobilization	Date, hour
<i>River side</i>	Side of the river where the tracked bottles is stranded and/or remobilized (north, south or island)	-
<i>Riverbank and vegetation typologies</i>	Characteristics of the stranding and/or remobilization site	-
Tidal and hydrometeorological conditions		
<i>Water flow*</i>	Water flow at start time (Q_i , in Montjean-sur-Loire, http://www.hydro.eaufrance.fr/)	m^3/s
<i>Water level</i>	Water levels at start time and at stranding (in St-Nazaire, http://maree.info/)	m
<i>Flood or ebb tides</i>	Flood or ebb tides at stranding (in St-Nazaire, http://maree.info/)	-
<i>Tidal ranges</i>	Tidal ranges at start time and at strandings (in St-Nazaire, http://maree.info/)	m

637

638